



Thermal conductivity of hypostoichiometric low Pu content (U,Pu)O_{2-x} mixed oxide

Christian Duriez*, Jean-Pierre Alessandri, Thierry Gervais,
Yannick Philipponneau

CEA Cadarache, DRN/DEC/SPU, 13108 St Paul Lez Durance, France

Received 21 January 1999; accepted 4 August 1999

Abstract

The 'laser flash' method was used to measure the thermal diffusivity of PWR mixed oxide fuels with Pu contents ranging from 3 to 15 wt% and oxygen to metal ratio (O/M) ranging from 2.00 to ~1.95. The temperature range extends from 700 to 2300 K. The fuel thermal conductivity is derived using heat capacity values of the mixed oxides calculated by Kopp's law from recommended values for the heat capacities of UO₂, PuO₂ and O₂. We observe an effect of the deviation from stoichiometry on the conductivity smaller than what is recommended for high plutonium content FBR fuel. Our results are fitted in the low temperature range to a classical phonon transport model. Abeles's simplified theory of phonon diffusion by point defects is used to discuss the results. We propose a new thermal conductivity relation, which takes into account the effect of the O/M ratio. © 2000 Elsevier Science B.V. All rights reserved.

PACS: 61.72.Ji; 66.70.+f; 44.10.+i; 44.50; 21.65.+f

1. Introduction

The thermal conductivity of mixed oxide (U,Pu)O₂ has been extensively reviewed [1–3]. These reviews were mainly concerned with high Pu content (~20% Pu, i.e., Pu/(U+Pu) ~0.2) mixed oxides for fast breeder reactors (FBR). The proposed recommendations following these reviews predict a strong decrease of the thermal conductivity when the mixed oxide becomes hypostoichiometric. The up-to-date recommendation [3], hereafter referred as the 'European FBR recommendation' is based on a re-analysis of the published experimental data restricted to 20% Pu content oxides. As a matter of fact, very few experimental results on the conductivity of hypostoichiometric low Pu content MOX fuel have been published [4]. Furthermore, recent diffusivity measurements done in our laboratory have shown that the recommendations for FBR fuels are not

adapted for low Pu content mixed oxides burned in pressurised water reactors (PWR). As PWR fuel may become hypostoichiometric during irradiation, accurate knowledge of the dependency of the thermal conductivity on the O/M ratio (O/M = number of oxygen atoms/number of heavy metal atoms) is required for in pile behaviour prediction. We have therefore realised new sets of diffusivity measurements to propose a recommendation adapted to PWR fuel.

2. Experimental

2.1. Sample preparation

We have prepared samples with Pu concentration of 3%, 6%, 10% and 15%. They are obtained by co-grinding of UO₂ and PuO₂ powders, pelletizing, and sintering at 1700°C for 4 h under moistened Ar + 5% H₂ atmosphere.

Electron probe microanalysis (EPMA) and X-ray diffraction (XRD) have shown that the obtained pellets

* Corresponding author.

E-mail address: duriez@drscad.ipsn.fr (C. Duriez).

present a non-homogeneous Pu concentration. Because the oxygen potential of mixed oxides depends on their Pu content, this would lead after reduction to some O/M variations across the material. As the O/M ratio is the main parameter of this study, we need samples with a uniform oxygen concentration and therefore mixed oxides with a uniform Pu concentration.

Homogenisation by annealing. To get samples with a homogeneous Pu concentration, the pellets were annealed for 240 h at 1700°C under the same atmosphere as for sintering. This atmosphere is chosen to maintain the pellets at the stoichiometric state ($O/M = 2.00$). We have shown by XRD that long annealing time is required for complete homogenisation of the Pu distribution, especially for the lowest Pu content.

XRD is used for lattice parameter determination. XRD spectra are obtained with a Phillips X-ray powder diffractometer on samples prepared by crushing pellet splinters and mixing the powder obtained in an epoxy resin. The lattice parameter is calculated from the spectra using at least 10 diffraction lines, giving a precision of 7×10^{-13} m. The results of XRD measurements are plotted in Fig. 1 as a function of the Pu content and the annealing time. It can be seen that for the lowest Pu contents (3% and 6%), the lattice parameter measured after sintering is close to the UO_2 value. It gets closer and closer to the Vegard's law as the annealing time increases, showing that a more homogeneous solid solution forms. For an annealing time of about 200 h at 1700°C, the lattice parameter follows the Vegard's law for all Pu contents. EPMA confirms that we obtain in that way more homogeneous solid solutions.

Table 1 gives the main characteristics of the different fuel batches prepared for the present study, before and after 240 h annealing.

Sample reduction. Pellets are cut into disks about 1 mm thick. About 3 disks from the same pellet are reduced together by heating in dry Ar + 5% H_2 at 1700°C.

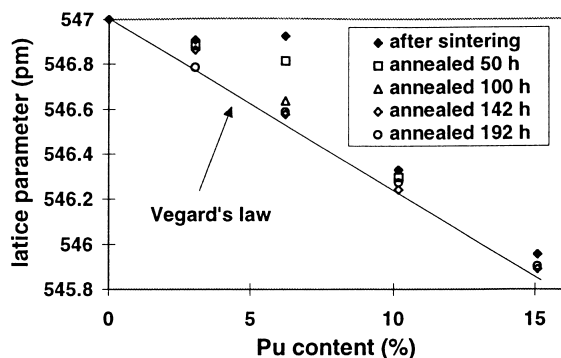


Fig. 1. Effect of annealing at 1700°C on the lattice parameter measured by XRD.

The O/M ratio after reduction is determined by XRD. A preliminary study with pellets from the same homogeneous batches has shown by coupling XRD lattice parameter measurements and thermogravimetric O/M determinations that the lattice parameter a varies linearly with the O/M ratio. We have observed no obvious dependence of the $da/d(O/M)$ coefficient on the Pu content, and we have obtained an average value $da/d(O/M) = 32 \times 10^{-12}$ m, in good agreement with previously published results analysed in Ref. [5, ch. 1], and with the 33×10^{-12} m value calculated by Ohmichi et al. [6]. Assuming an uncertainty of $\pm 1 \times 10^{-12}$ m on the $da/d(O/M)$ coefficient and taking into account that the precision on the lattice parameter measurement is 7×10^{-13} m, the uncertainty on the O/M determination by XRD is about $\pm 3 \times 10^{-3}$.

We have used different reduction times. Fig. 2 presents the reached O/M ratios, as calculated from the XRD lattice parameter determinations, versus the heating time at 1700°C. We obtained very low reduction kinetic compared to what could be expected from the work of Bayoglu [7]. Even for a treatment as long as 400 min, the reduction limit (which corresponds to a state where all the Pu cations are trivalent) is not reached, except for the 3% Pu batch.

As the oxygen potential of our reducing atmosphere should be sufficiently low to reach this reduction limit for all Pu contents, it is unlikely that thermodynamic equilibrium is reached, except for the 400 min treatment of the 3% Pu samples. It is then possible to have an O/M gradient across the sample disks if the reduction kinetic is limited by oxygen diffusion. To assess this hypothesis, we performed a reduction treatment with a full pellet (12 mm high, 8.4 mm in diameter) in conditions where such an O/M gradient should most probably occur: 15% Pu content, 60 min reduction time. We then cut the

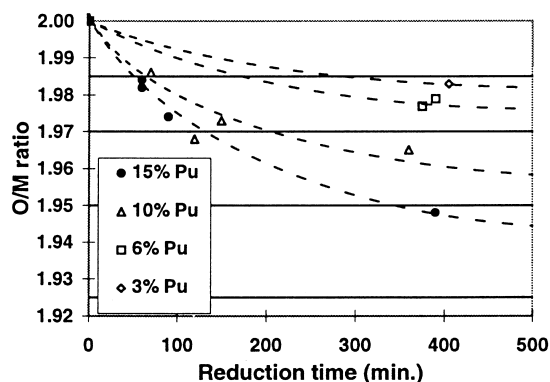


Fig. 2. O/M ratios determined from XRD lattice parameter measurements versus the reduction time. Dashed lines give the reduction limits (all Pu cations are trivalent) that are $O/M = 1.985, 1.97, 1.95$ and 1.925 for Pu content = 3%, 6%, 10% and 15%, respectively.

Table 1
Main characteristics of the reference fuels used for the present study

Expected Pu content	3%	6%	10%	15%
Measured Pu content (wt%)	3.06 ± 0.06	6.22 ± 0.12	10.18 ± 0.2	15.10 ± 0.2
Theoretical density d_{th} (10^3 kg m ⁻³)	10.964	10.979	10.984	10.993
Measured density d_m (10^3 kg m ⁻³)				
Before annealing	10.51 ± 0.01	10.47 ± 0.01	10.53 ± 0.01	10.52 ± 0.01
After annealing	10.55	10.57	10.54	10.50
d_m/d_{th}				
Before annealing	95.9	95.4	95.8	95.7
After annealing	96.1	96.2	95.9	95.6
Mean grain size (μ m)				
Before annealing	6	5.1	5.8	5.4
After annealing	15.2	22.8	16.1	18.9

pellet to set apart 2 samples from the centre and the periphery of the pellet. XRD measurements gave no evidence of an O/M gradient: we obtained for both samples an O/M ratio of 1.981 in good agreement with the value 1.983 obtained previously with the 15% Pu disks reduced during 60 min. Then, the reduction kinetic is likely to be controlled by surface reactions.

Such a slow oxygen exchange rate between solid and gas was not expected [7]. A possible explanation could be the particular microstructure of our samples, due to the long annealing treatment (240 h at 1700°C): mean grain size increases by a factor of 3–4 during the treatment. Consequently, the number of ridge sites, which are known to be preferential sites for oxygen adsorption and dissociation is much lower after treatment.

2.2. Diffusivity measurements

We used the laser flash method to perform diffusivity measurements.

The schematic layout of the device is given in Fig. 3. The laser is a ~30 J/pulse YAG laser. The pulse duration is about 1 ms. High frequency induction is used to heat the sample. The atmosphere of the heating chamber is nitrogen (2 mbar absolute pressure), renewed at 800 l/h. The temperature of the sample is measured by optical pyrometers. The pyrometers, located outside of the glove box, are calibrated by comparison with a W–Re thermocouple. The temperature rise after the laser shot is recorded by an In–Sb photodetector, interfaced with a computer via a numeric oscilloscope. Diffusivity is calculated from the signal using Degiovanni's thesis model [8].

For each set of diffusivity measurements, at least 2 sample disks are used. The temperature range 400–2000°C is covered, with roughly one temperature step each 50–100°C. For each temperature step, 2 shots are performed. Few measurements were done during cool-

ing to check for any modification of the O/M ratio upon heating. As the diffusivity depends on the O/M ratio, such a modification would result in a change of the diffusivity values at low temperature. This was never observed during the present work. Furthermore, for one sample (15% Pu, 60 min reduction time), we have confirmed by a second XRD measurement that no modification of the O/M ratio occurred during the diffusivity measurements.

Before the measurements with reduced samples, we first performed measurements with stoichiometric ones.

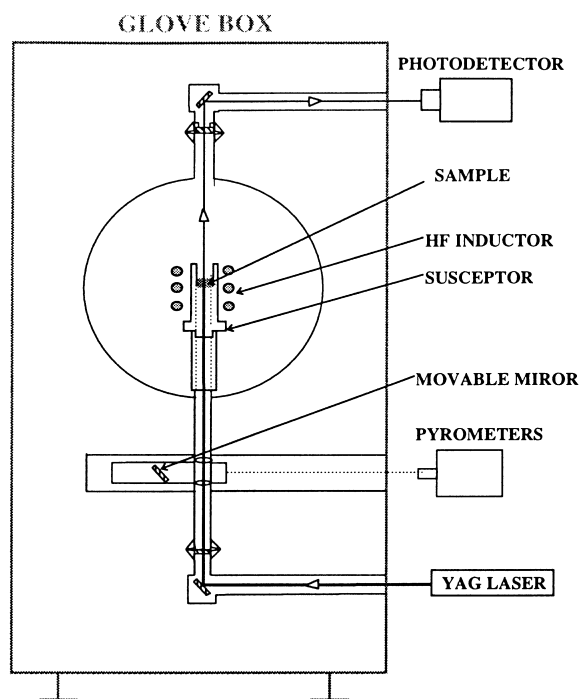


Fig. 3. Schematic layout of the laser flash apparatus.

To be sure their O/M ratio is 2.00, the disks underwent a heat treatment (3 h at 900°C under Ar + 5% H₂ atmosphere, water saturated at 20°C). The oxygen potential ΔG_{O_2} of this gas mixture is about -115 kcal/mol at 900°C, which, for any plutonium concentration, lies in the range of oxygen potential required to obtain, at thermodynamic equilibrium and 900°C, stoichiometric (U,Pu)O₂ mixed oxides [9].

The results of diffusivity measurements (not presented here) show that the diffusivity decreases when the mixed oxide becomes hypostoichiometric, as expected. The decrease is more pronounced at low temperature.

For further quantitative analysis, the results are converted into thermal conductivity.

3. Thermal conductivity calculation

Thermal conductivity data are calculated from diffusivity measurements by the relation: $\lambda(T) = f(p)/f(0.05)a(T)\rho(T)C_p(T)$, where

$\lambda(T)$	thermal conductivity at temperature T and for 95% theoretical density ($\text{W m}^{-1} \text{K}^{-1}$)
$f(p)$	porosity correction factor (p is the fractional porosity)
$a(T)$	diffusivity measured at temperature T ($\text{m}^2 \text{s}^{-1}$)
$\rho(T)$	density at temperature T (kg m^{-3})
$C_p(T)$	specific heat at constant pressure for temperature T ($\text{J kg}^{-1} \text{K}^{-1}$)

For the porosity effect correction, the modified Maxwell-Eucken relation is used: $f(p) = (1 + 2p)/(1 - p)$. By multiplying by $f(p)/f(0.05)$, we obtain a conductivity equivalent to a 95% theoretical density fuel from diffusivity results obtained with samples of porosity p . In that way, we can compare results from different batches having different values of porosity. Also this porosity correction has to be made for comparison with reference recommendations. Note that because our samples are in any case close to 95% theoretical density, the correction is small and thus depends very little on the chosen model.

For $\rho(T)$, we use the measured density at room temperature by immersion in cyclohexane and Martin's recommended relation for the thermal expansion [10].

For C_p , we performed a specific study by differential scanning calorimetry (DSC) with stoichiometric samples from the same batches than those used for the diffusivity measurements [11]. The maximum temperature for our DSC apparatus is 1300°C. The results obtained in the temperature range 200–1300°C were in very good agreement (within 2–3%) with the Kopp's law used by Philipponneau [3], that is,

$$C_p[(U_yPu_{1-y})O_2] = yC_p[UO_2] + (1 - y)C_p[PuO_2]$$

with

$$C_p[UO_2] \text{ (J g}^{-1} \text{K}^{-1}\text{)} = 46.776 + 0.10015T - 1.0045 \times 10^{-4}T^2 + 4.2386 \times 10^{-8}T^3 - 50.145 \times 10^{-12}T^4,$$

$$C_p[PuO_2] \text{ (J g}^{-1} \text{K}^{-1}\text{)} = 91.526 + 3.184 \times 10^{-6}T^2 - 2.269 \times 10^6/T^2.$$

For hypostoichiometric samples we subtract a small corrective term:

$$C_p[(U_yPu_{1-y})O_{2-x}] = C_p[(U_yPu_{1-y})O_2] - x/2C_p[O_2]$$

with

$$C_p[O_2] \text{ (J g}^{-1} \text{K}^{-1}\text{)} = 27\,849 + 8.53 \times 10^{-3}T - 2.0454 \times 10^{-6}T^2 + 1.932 \times 10^{-10}T^3.$$

This Kopp's law is validated for low Pu content MOX fuel only up to 1300°C (1573 K). We assume that this law is still valid at higher temperature to calculate our conductivity data up to 2000°C.

The results obtained for the stoichiometric fuels are plotted in Fig. 4 for all Pu contents, and compared with the European recommendation for conductivity of fast breeder reactor (FBR) fuel (Ref. [5, ch. 7]), the Martin recommendation [2] and the Harding and Martin recommendation for UO₂ [12]. It can be seen that the conductivity seems not to depend on the Pu concentra-

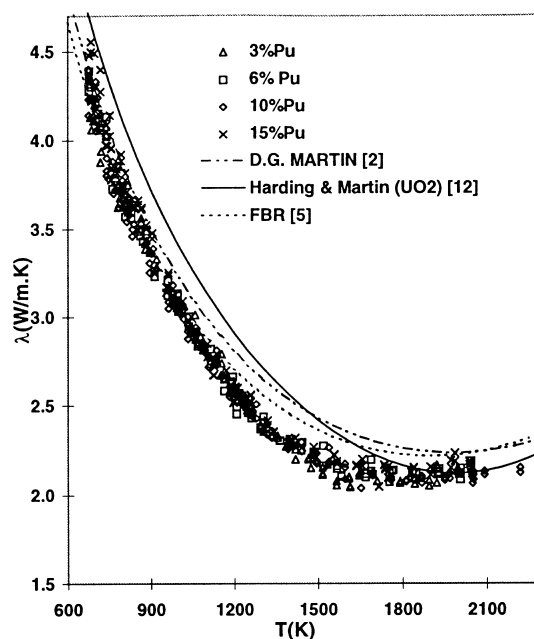


Fig. 4. Conductivity data for the stoichiometric reference mixed oxide fuels.

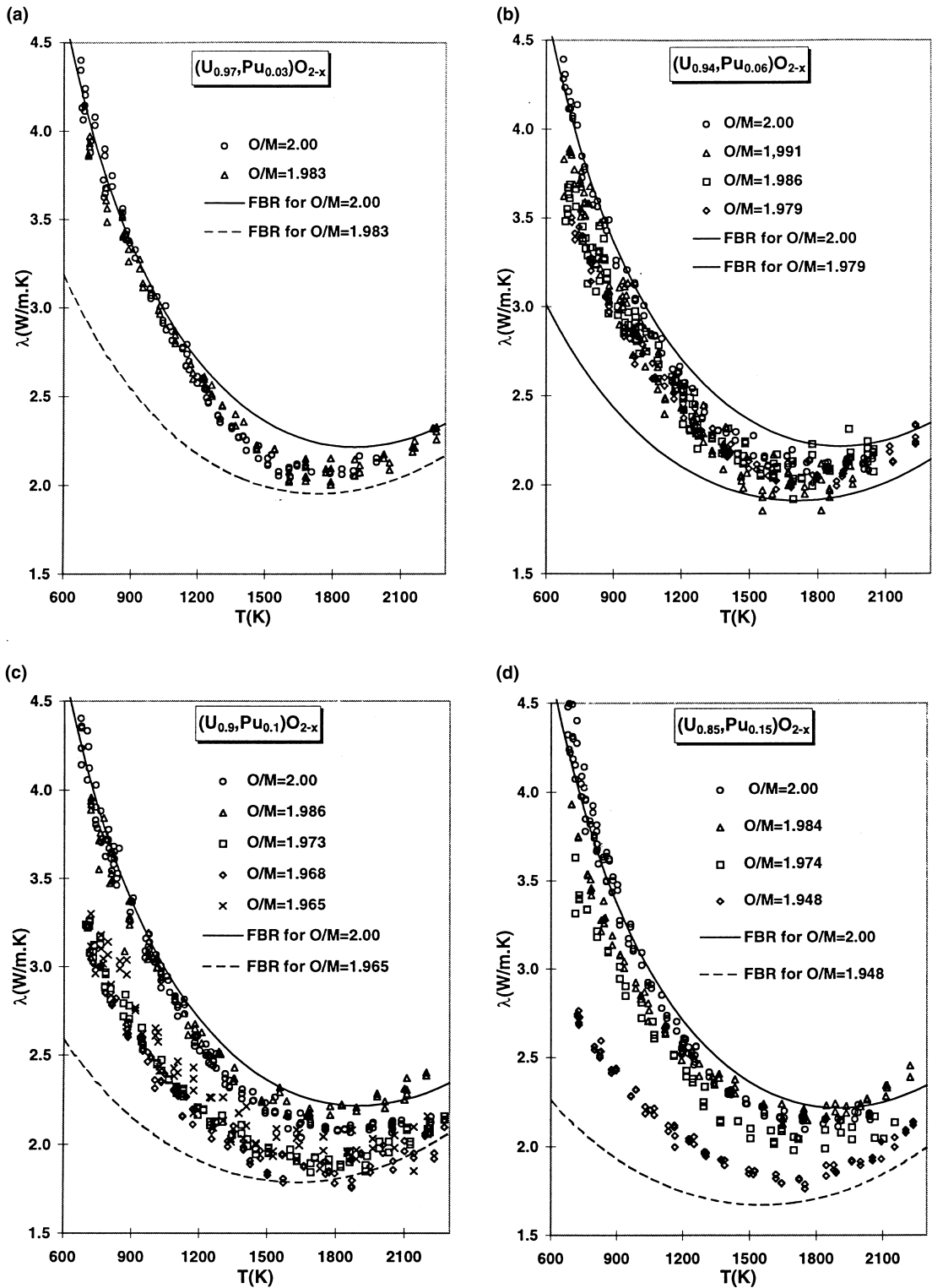


Fig. 5. Conductivity data calculated from diffusivity measurements for 3%, 6%, 10% and 15% Pu content MOX fuel, respectively.

tion. In the low temperature range, both the FBR and the Martin recommendations agree quite well with the experimental data for the stoichiometric fuels. At high temperature, they both overestimate the data. Over the whole temperature range, the data are significantly lower than the Harding and Martin UO₂ recommendation, indicating that even a small amount of Pu leads to a decrease of the conductivity.

The results are presented for each investigated Pu content in Fig. 5(a)–(d). We have also plotted in these figures the FBR European recommendation for O/M = 2.00 and for the lowest O/M ratio reached. The conductivity decrease at low temperature when the fuel becomes hypostoichiometric is smaller than the prediction given by the FBR recommendation.

4. Quantitative analysis

To perform a quantitative analysis of these results, we first restrict to the temperature range in which the Kopp's law used for specific heat has been validated, that is $T < 1573$ K. In this temperature range, the oxide conductivity is mainly due to phonon transport. Bonnerot [4] has shown that below 1300 K, other contributions can be neglected for (U,Pu)O₂ mixed oxides. We therefore limit our quantitative analysis to this maximum temperature.

We use a classical phonon heat transport model to fit our data points, that is, $\lambda(T) = 1/(A + BT)$, where T is the temperature in Kelvin, A a term due to phonon interactions with the lattice defects and B takes into account the phonon–phonon interactions.

For each set of measurements, we perform a linear regression on $1/\lambda(T)$ data points for $T < 1300$ K. Values of A and B coefficients thus obtained are presented in Table 2 and plotted in Figs. 6–9.

The last column of Table 2 gives the correlation coefficients of the linear fits. The values are close to 1, showing that the chosen model suits well to describe our results, at least for $T < 1300$ K. The best results are obtained for the stoichiometric samples, indicative of a lower dispersion of the measurements.

Values of coefficients A and B are plotted versus the Pu concentration in Figs. 6 and 7, respectively, for stoichiometric samples and for samples around O/M = 1.985. Our results are compared to those of Bonnerot [4]. As far as we are aware, Bonnerot's work, which was performed in our laboratory during 1986–1987, is the only published study where thermal conductivity for low Pu content, hypostoichiometric (U,Pu)O_{2-x} mixed oxides has been systematically investigated. Our present results are also compared to the European recommendation for FBR mixed oxide fuel [5]. This recommendation gives no dependence of the A value with the Pu content. Our results appear

Table 2

Results of the linear regressions on resistivity data points (for $T < 1300$ K)

%Pu	O/M (± 0.03)	$A \times 10^{-2}$ m K W ⁻¹	$B \times 10^{-4}$ m W ⁻¹	Correlation coefficient
3	2.00	3.96	2.875	0.990
	1.983	7.25	2.559	0.990
6	2.00	3.27	2.96	0.991
	1.991	5.90	2.897	0.955
	1.986	9.60	2.562	0.952
	1.979	10.45	2.566	0.988
10	2.00	3.96	2.894	0.990
	1.986	8.14	2.490	0.976
	1.973	11.16	2.877	0.986
	1.968	12.50	2.846	0.974
	1.965	12.10	2.676	0.915
15	2.00	2.17	3.039	0.990
	1.984	8.12	2.645	0.986
	1.974	10.81	2.525	0.987
	1.948	18.95	2.489	0.983

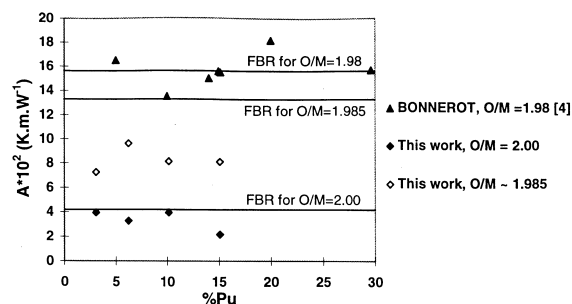


Fig. 6. Coefficient A versus the Pu content. Horizontal lines indicate values recommended for FBR mixed oxide in [5].

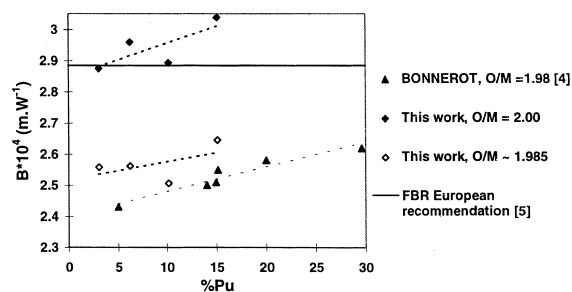


Fig. 7. Coefficient B versus the Pu content. Dashed lines are linear regressions on the data points.

to be consistent with this assumption. For the stoichiometric fuel, our results are in good concordance with the A value recommended in [5]. On the other

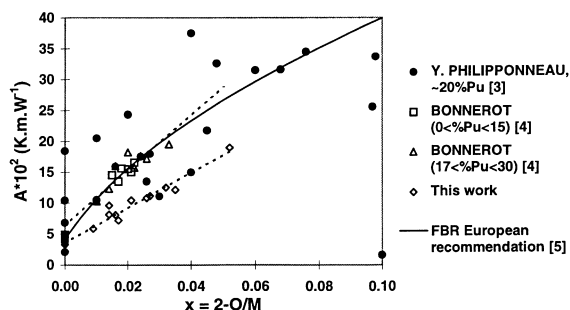


Fig. 8. Coefficient A versus the deviation from stoichiometry. The upper dashed line is a linear regression on Bonnerot's results. The lower one is a linear regression on our present results.

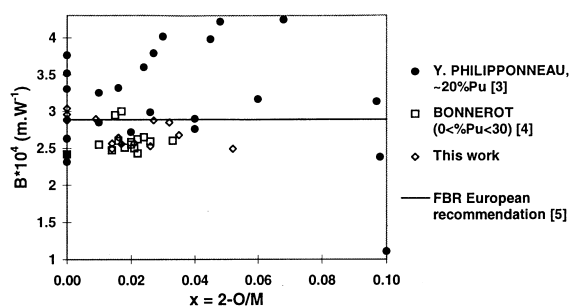


Fig. 9. Coefficient B versus the deviation from stoichiometry.

hand, for the hypostoichiometric samples, we observe an increase of A smaller than what is recommended for FBR 20% Pu mixed oxides [5]. It can be seen that previous results of our laboratory [4], on samples with Pu concentrations ranging from 5% to 30% also showed a strong increase of A when the mixed oxides become hypostoichiometric, even for the low Pu concentrations. But it should be pointed out that, because of the fabrication process, the Pu distribution was less homogeneous for these old low Pu content batches.

Fig. 7 shows that we observe, like in our older results [4], a slight increase of B with the Pu concentration. This might be explained by the inelastic phonon interaction model of Liebfried et al. [13]. However, this increase is small compared to the change of B value when the O/M ratio changes.

In Fig. 8, we have plotted coefficient A versus the deviation x from stoichiometry, without distinction of the Pu concentration as no strong variation of A versus the Pu content was observed. Our results are compared to our older ones [4] and to the values of A issued from the analysis of Philipponneau [3]. This extensive analysis of published results on $(U_{0.8}, Pu_{0.2})O_{2-x}$ fuels has concluded to a parabolic dependency of A with the deviation from stoichiometry, the increase of A slowing down

for high deviation. But it should be pointed out that the A values issued from the work of Philipponneau [3] are highly dispersed, probably partly because many different experimental works are involved. We do not observe in the investigated range such a parabolic dependency. We rather observe, like previously [4], a linear variation of coefficient A with x . But the slope of this variation is much lower than what was observed by Bonnerot [4], even for the low Pu content samples. The discrepancy may come, as already pointed out, from the less homogeneous Pu distribution of the low Pu content samples prepared in our laboratory in 1986–1987. For this reason, we think that our recent data are more confident for this low Pu content range than the older Bonnerot's data. Thus, we conclude that the effect of the deviation from stoichiometry on the conductivity of $(U,Pu)O_2$ mixed oxides is less important for low Pu concentrations (<15%) than for high Pu concentrations (20–30%) FBR fuels.

Coefficient B is plotted versus the deviation from stoichiometry in Fig. 9. Again, our results are compared to those of Bonnerot [4] and Philipponneau [3]. Again, it can be noticed that the values from the analysis of Philipponneau [3] are highly dispersed. Because of this high dispersion, it was proposed to use a constant value of B to describe the conductivity of FBR fuel [3,5]. Even if our dispersion is still quite high, it is obvious that our B values are on average lower for the hypostoichiometric samples than for the stoichiometric ones. For these stoichiometric samples, the values obtained for B are close to the value recommended for stoichiometric FBR fuels [5].

5. Discussion

The simple relationship $\lambda = 1/(A + BT)$ used to fit our data up to 1300 K corresponds to a model based on weak scattering of phonons by point defects, widely used to describe the thermal conductivity of dielectric solids above their Debye temperature. A is the lattice defect thermal resistivity, due to the phonon interactions with the lattice defects and BT corresponds to the intrinsic lattice thermal resistivity caused by phonon–phonon interactions (Umklapp process).

5.1. Lattice defect thermal resistivity

Ambegaoker [14] expressed the term A as

$$A = \frac{\pi^2 \bar{V} \theta_D}{3\bar{v}h} \sum_i \Gamma_i = C \sum_i \Gamma_i,$$

where \bar{V} is the mean atomic volume in the lattice, θ_D the Debye temperature, \bar{v} the mean phonon velocity, h the Plank's constant and Γ_i is a cross-section parameter for

phonon scattering by point defect i . Abeles [15], expressed Γ_i as the result of mass and size effects:

$$\Gamma_i = X_i \left[\left(\frac{\bar{M} - M_i}{\bar{M}} \right)^2 + \varepsilon \left(\frac{\bar{r} - r_i}{\bar{r}} \right)^2 \right].$$

X_i is the atomic fraction of the point defect i , M_i its mass and r_i its atomic radius, \bar{M} is the mean atomic mass of the lattice and \bar{r} the mean atomic radius of the lattice. $\varepsilon = 32(1 + 1.6\gamma)^2$ (γ is the Grüneisen constant) is a parameter representing the magnitude of the strain generated in the lattice by the size difference. As many simplifying assumptions are needed to obtain this relationship, Abeles proposes to use ε as an adjustable parameter.

The sum $\sum \Gamma_i$ may be written as

$$\sum_i \Gamma_i = \left(\frac{\sum_i X_i M_i^2 - \bar{M}^2}{\bar{M}^2} \right) + \varepsilon \left(\frac{\sum_i X_i r_i^2 - \bar{r}^2}{\bar{r}^2} \right).$$

When a new species is added and goes in solution in the lattice, new point defects are created. Then, the lattice defect thermal resistivity A increases by ΔA . This increase can be expressed by the difference:

$$\Delta A = A_{ss} - A_{ini} = C_{ss} \sum_j \Gamma_j - C_{ini} \sum_i \Gamma_i,$$

where the subscripts ss and ini stand for the solid solution and the initial material respectively. Subscript j means that the sum is on all the point defect of the solid solution and i is for the point defects of the initial lattice. This approach has been used by several authors to interpret results of conductivity measurements on actinides based fluorite type solid solutions [16–25]. We will use this approach to calculate the A increase when the (U,Pu)O₂ mixed oxide becomes hypostoichiometric.

We consider the initial matrix to be the stoichiometric mixed oxide and the reduced oxide to correspond to a solid solution of oxygen vacancies in the initial lattice. We then use the subscripts 2.00 and 2– x instead of ini and ss, respectively.

We deal with ionic crystals and the phonon scattering centres are in our case:

- for the stoichiometric oxide (U_(1–y),Pu_y)O₂: the U⁴⁺, Pu⁴⁺ cations and the O^{2–} anions.
- for the hypostoichiometric oxide (U_(1–y),Pu_y)O_{2–x}: U⁴⁺, Pu⁴⁺, O^{2–}, Pu³⁺ and O_v (oxygen vacancy).

To simplify the writing, we will further use the subscripts 1–5 for the species U⁴⁺, Pu⁴⁺, O^{2–}, Pu³⁺ and O_v, respectively.

From electric neutrality considerations, we can calculate the atomic fractions to be:

- in the stoichiometric oxide: $Y_1 = (1 - y)/3$, $Y_2 = y/3$ and $Y_3 = 2/3$.
- in the hypostoichiometric oxide: $X_1 = (1 - y)/3$, $X_2 = (y - 2x)/3$, $X_3 = (2 - x)/3$, $X_4 = 2x/3$ and $X_5 = x/3$.

Because the deviation from stoichiometry is small, that is to say $(x/2) \ll 1$, we will make the following assumptions:

- The atomic radius of a given species is the same in the stoichiometric and the hypostoichiometric oxide. Indeed, the mean coordination numbers of cations are 8 and $8 - 4x$ in the stoichiometric and the hypostoichiometric oxide, respectively, and according to Ohmichi et al. [6], the mean ionic radius of cation with $8 - 4x$ mean coordination number is approximately $r - 0.02x$ if r is its ionic radius for 8 coordination number. This leads to a radius decrease of about 1% for $x = 0.05$, which is close to the maximum deviation from stoichiometry we have reached in this study. In fact, even if small, this effect will be taken into account in the calculation through assigning an apparent value to the oxygen vacancy radius.
- The mean atomic mass and mean atomic radius of the lattice do not change when the oxide becomes hypostoichiometric. Indeed, from O/M = 2.00 to O/M = 1.95, the relative mean mass change is about 0.025% and the relative mean radius change is less than 0.5% (calculated from a lattice parameter change $\Delta a/\Delta x = 0.032$ nm).
- The C constant is the same for the stoichiometric and the hypostoichiometric oxide (i.e., $C_{2.00} = C_{2-x} = C$). According to Fukushima et al. [20], we used the relation $C_{2-x} = C_{2.00}(a_{2-x}/a_{2.00})^2$ ($a_{2.00}$ and a_{2-x} are the lattice parameters of the stoichiometric and the hypostoichiometric oxides, respectively) to show that the difference in the C constant is on the order of 0.5% between the stoichiometric oxide and the oxide reduced to O/M = 1.95.

Admitting these assumptions, we can then write

$$\begin{aligned} \frac{A_{2.00}}{C} &= \sum_{i=1}^3 \Gamma_i \\ &= \left(\frac{\sum_{i=1}^3 Y_i M_i^2 - \bar{M}^2}{\bar{M}^2} \right) + \varepsilon \left(\frac{\sum_{i=1}^3 Y_i r_i^2 - \bar{r}^2}{\bar{r}^2} \right), \end{aligned}$$

$$\begin{aligned} \frac{A_{2-x}}{C} &= \sum_{j=1}^5 \Gamma_j \\ &= \left(\frac{\sum_{j=1}^5 X_j M_j^2 - \bar{M}^2}{\bar{M}^2} \right) + \varepsilon \left(\frac{\sum_{j=1}^5 X_j r_j^2 - \bar{r}^2}{\bar{r}^2} \right) \end{aligned}$$

and the difference $\Delta A = A_{2-x} - A_{2.00}$ becomes

$$\begin{aligned} \Delta A &= C \left\{ \frac{1}{\bar{M}^2} \left[\sum_{i=1}^3 (X_i - Y_i) M_i^2 + X_4 M_4^2 + X_5 M_5^2 \right] \right. \\ &\quad \left. + \frac{\varepsilon}{\bar{r}^2} \left[\sum_{i=1}^3 (X_i - Y_i) r_i^2 + X_4 r_4^2 + X_5 r_5^2 \right] \right\}, \end{aligned}$$

which leads to

$$A_{2-x} = C \left\{ -\frac{M_3^2}{\bar{M}^2} + \frac{\varepsilon}{\bar{r}^2} [2(r_4^2 - r_2^2) + (r_5^2 - r_3^2)] \right\} \frac{x}{3} + A_{2.00}. \quad (1)$$

We find that ΔA increases linearly with the deviation from stoichiometry x and does not depend on the plutonium content y . This is consistent with the experimental results and is a good indication that Abeles simple theory is well suited to describe our results. The strain effect on the lattice comes from replacement of Pu^{4+} cations by Pu^{3+} (the difference $r_4^2 - r_2^2$) and replacement of oxygen anions by vacancies (the difference $r_5^2 - r_3^2$).

Identification with the slope $dA/dx = 2.85 \text{ m K W}^{-1}$ obtained from a linear regression on the experimental A values (see Section 6) leads to

$$\varepsilon = \frac{\bar{r}^2}{2(r_4^2 - r_2^2) + (r_5^2 - r_3^2)} \left(\frac{3}{C} \frac{dA}{dx} + \frac{M_3^2}{\bar{M}^2} \right). \quad (2)$$

For the ionic radius of Pu^{4+} and O^{2-} , we use the values reported by Shanon [26], that are $r_2 = 0.096 \text{ nm}$ and $r_3 = 0.1368 \text{ nm}$, respectively. The ionic radius of Pu^{3+} has been estimated by Ohmichi et al. to be $r_4 = 0.110 \text{ nm}$ [6]. These authors have also estimated the oxygen vacancy radius: $r_5 = 0.15 \text{ nm}$. According to them, this value has to be corrected to an apparent value r_5^* to take into account the change in ionic radius of cations due to these oxygen vacancies. They give the relationship $r_5^* = r_5 + 2\beta$, where $\beta = \sum X_i (\Delta r_i / \Delta x)$. The sum is on the cations (i.e., $i = 1, 2$ and 4) and $\Delta r_i / \Delta x$ represents the change of cations radius due to the change in their coordination number. Using the value $\Delta r_i / \Delta x = -0.02 \text{ nm}$ given by Ohmishi et al., we find $r_5^* = 0.1367 \text{ nm}$.

To calculate the mean atomic mass \bar{M} , we take into account the isotopic composition of the uranium and plutonium used. For the plutonium content, we use a mean value $y = 8.5\%$ but \bar{M} as well as \bar{r} depend very little on the Pu content (less than 0.1% variation for the Pu content range investigated).

To evaluate the C constant for the mixed oxide (U, Pu) O_2 (we use hereafter the subscript MOX), we start from the value for UO_2 : we take for the Debye temperature the value $\theta_D = 242 \text{ K}$ reported for UO_2 by Willis [27], and for the mean phonon velocity the value reported by Ainscough and Wheeler [28], that is $\bar{v} = 4.3 \times 10^3 \text{ m/s}$. The mean atomic volume is obtained from the lattice parameter a of UO_2 , that is to say $\bar{V} = a^3/12 = 13.64 \times 10^{-30} \text{ m}^3$. Therefore, the C value for UO_2 is calculated to be $C_{\text{UO}_2} = 0.886 \text{ m K W}^{-1}$. For two isomorphous compounds, the C constants can be related by [20]

$$\frac{C_{\text{MOX}}}{C_{\text{UO}_2}} = \left(\frac{a_{\text{MOX}}}{a_{\text{UO}_2}} \right)^2.$$

We then obtain a value $C_{\text{MOX}} = 0.884 \text{ m K W}^{-1}$ very close to the UO_2 value.

Finally, the relation (2) gives $\varepsilon = 25.85$. This value is about four times lower than the values observed for stoichiometric solid solutions of actinide oxide containing rare earth elements or other actinides [16–25]. This indicates that the strain caused on the (U,Pu) O_2 lattice when creating oxygen vacancies is much smaller than the strain generated in an actinide oxide lattice when adding in solution a foreign element.

However, it can be shown from Eq. (1) that the strain effect on the additional thermal resistivity is the dominating effect. The mass effect goes toward a decrease of the resistivity, but is in fact negligible, as it represents less than 0.3% of the strain effect.

5.2. The intrinsic lattice thermal resistivity

The intrinsic lattice thermal resistivity of dielectric solids can be estimated by the relationship of Liebfried et al. [13]:

$$B = \gamma^2 / \left(\frac{24}{10} 4^{1/3} (h/k)^3 \bar{M} \bar{V}^{1/3} \theta_D^3 \right), \quad (3)$$

where γ is the Grüneisen constant and k the Boltzmann constant.

Eq. (3) has been shown to predict B values 3 or 4 times lower than experimentally determined values, but can be used to evaluate the B value of a given compound relative to a known B value of an isomorphous compound, as first done by Gibby [16]. Using the Lindeman [29] relationship which express θ_D as a function of the melting temperature, Gibby has given the B values ratio of two isomorphous compounds 1 and 2:

$$\frac{B_2}{B_1} = \left(\frac{M_2}{M_1} \right)^{1/2} \left(\frac{a_2}{a_1} \right)^2 \left(\frac{T_{M1}}{T_{M2}} \right)^{3/2} \left(\frac{\gamma_1}{\gamma_2} \right)^2, \quad (4)$$

where M_i , a_i , T_{Mi} and γ_i are respectively the molecular weight, the lattice parameter, the melting temperature and the Grüneisen constant for the compound i .

Considering compounds 1 and 2 to be the (U,Pu) O_2 and (U,Pu) O_{2-x} solid solution, respectively, and assuming that the Grüneisen constant is the same for these two compounds, the variation of the intrinsic lattice thermal resistivity with the deviation from stoichiometry x can be evaluated from Eq. (4). We use for the melting temperature of the stoichiometric and hypostoichiometric mixed oxides the liquidus temperatures, evaluated from the results of Lyon and Baily [30] and those of Aitken and Evans [31]. We use for the lattice parameter the value $da/dx = 32 \times 10^{-12} \text{ m}$ (see Section 2.1, Sample reduction). Thus, we obtain a B value constant within 1% over the investigated O/M range ($1.95 < \text{O/M} < 2.00$). Experimentally, we rather observe a decrease of B when the samples become hypostoichiometric and we will see in

Section 6 that our conductivity data are better fitted when assuming a linear decrease of the B parameter instead of a constant value. However, because of the high dispersion on the experimental B values, it is difficult to definitely conclude.

6. Conductivity relation

The aim here is to provide a simple relationship to describe the thermal conductivity of PWR low Pu content mixed oxide fuels and its variation with deviation from stoichiometry.

6.1. The phonon conduction domain

A simple phonon conduction model ($\lambda = 1/(A + BT)$) has been shown to be well suited to fit our results for $T < 1300$ K. On the basis of the analysis of Sections 4 and 5, we make the following assumptions:

- Coefficients A and B are independent of the Pu concentration. In fact, there is a small dependence, but we neglect it compared to the variation with the O/M ratio.
- Coefficient A increases linearly with the deviation from stoichiometry.

To obtain a relationship between the coefficient A and the deviation from stoichiometry, we perform a linear regression on the values of coefficient A . It gives $A(x) = 2.85x + 0.035$ m K W⁻¹ and a correlation coefficient $R = 0.978$.

To set B , two different choices are tried:

- B is constant and equal to the mean of all values.
- B decreases linearly with the deviation from stoichiometry and the $B(x)$ relationship is obtained by linear regression.

These two different ways of setting B are applied either on initial values of B or on values recalculated after setting the A coefficient on the line $A(x) = 2.85x + 0.035$ m K W⁻¹. Thus, four options have to be tested.

Two additional options are tested: new values of coefficient A are calculated after setting the coefficient B either at a constant mean value or on the straight line given by the linear regression on the initial values, that is $B(x) = (-7.21x + 2.85) \times 10^{-4}$ m W⁻¹.

So, six different options have been quantitatively compared with the experimental data: we consider that the experimental data are well described up to 1300 K by their initial fit (given in Table 2) and we calculate the relative mean difference between a given tested option and the fits by the relation

$$\langle \Delta\lambda/\lambda \rangle = \frac{1}{N} \sum_{T=700 \text{ K}}^{1300 \text{ K}} |\lambda_{\text{fit}} - \lambda_{\text{model}}|/\lambda_{\text{fit}}$$

with T varying by 20° steps (i.e., $N = 31$).

Thus, 6×15 $\langle \Delta\lambda/\lambda \rangle$ values are calculated (15 being the number of experimental data sets). These calculations lead to the following conclusions:

- To recalculate the B parameter after the A parameter is set on the straight line $A(x) = 2.85x + 0.035$ m K W⁻¹ changes only slightly the B values.
- To recalculate the A parameter after setting the B parameter improves the results only if the B parameter was set at a constant value.
- The choice of a constant value for B does not give satisfactory results for the stoichiometric samples data sets. This is shown in Table 3, which gives the results for the two options that have used the recalculated B values: the first line corresponds to the option setting a constant mean B value, the second line corresponds to the option setting B on the decreasing straight line given by linear regression, that is, $B(x) = (-7.15x + 2.86) \times 10^{-4}$ m W⁻¹.

Finally, over the six tested options, the best results are obtained for the following:

- A is given by a linear regression on the initial values, that is, $A(x) = 2.85x + 0.035$ m K W⁻¹.
- B is given by a linear regression on the values recalculated after setting $A(x) = 2.85x + 0.035$ m K W⁻¹, that is, $B(x) = (-7.15x + 2.86) \times 10^{-4}$ m W⁻¹.

For this option, the relative mean difference with the fits rarely exceeds 5%, which is in the range of the absolute uncertainty associated with the diffusivity measurement method, mainly due to the uncertainty of the sample temperature determination. We should also have in mind the uncertainty associated with the O/M determination (see Section 2, sample reduction). Only the [3% Pu, O/M = 1.983] set is not well described, giving a mean difference $\langle \Delta\lambda/\lambda \rangle = 8.15\%$. This expresses the fact that the results obtained for this reduction are very close to those obtained with the stoichiometric samples: the conductivity decrease is much lower than what could be expected from results obtained with the higher Pu content batches. New measurements with very low Pu content batches should be performed.

Despite this problem and despite the fact that there is no theoretical evidence for a decrease of B with the deviation from stoichiometry, we propose to retain the following relation to describe the phonon thermal conductivity of PWR low Pu content mixed oxides:

$$\lambda_{\text{ph}} = 1/(A + BT) \quad (5)$$

with

$$A = A(x) = 2.85x + 0.035 \text{ m K/W},$$

$$B = B(x) = (-7.15x + 2.86) \times 10^{-4} \text{ m/W}.$$

Table 3
Relative mean differences $\langle \Delta\lambda/\lambda \rangle$ (in %), calculated in the range 700–1300 K (see text), between two tested relations and the fits on the experimental data for the reference batches

% Pu	3% Pu	6% Pu	10% Pu	15% Pu	Mean $\langle \Delta\lambda/\lambda \rangle$									
O/M	2.00	1.983	2.00	1.991	1.986	1.979	2.00	1.986	1.968	1.965	2.00	1.984	1.974	1.948
$\langle \Delta\lambda/\lambda \rangle^a$	6.12	7.97	6.58	4.37	1.35	1.84	6.74	5.03	3.62	2.5	4.81	2.29	5.67	3.91
$\langle \Delta\lambda/\lambda \rangle^b$	1.94	8.15	2.38	2.33	0.99	1.22	2.53	5.76	5.33	5.2	1.87	2.75	4.1	1.45

^a $A(x) = 2.85x + 0.035 \text{ m K W}^{-1}$ and $B = \langle B_{\text{recalculated}} \rangle = 2.716 \times 10^{-4} \text{ m W}^{-1}$.

^b $A(x) = 2.85x + 0.035 \text{ m K W}^{-1}$ and $B(x) = (-7.115x + 2.86) \times 10^{-4} \text{ m W}^{-1}$.

6.2. Extension of the temperature range

The relation $\lambda = 1/(A + BT)$, based on a phonon conduction model, cannot account for conductivity at high temperature, where electronic and radiative mechanisms contribute to the heat transport. Following Bonnerot [4], we have first limited our data fits to a maximum temperature of 1300 K. Then, we take up again the linear regressions on the resistivity data using a variable maximum temperature for the regression instead of 1300 K. We start from a regression maximum temperature of 1000 K and we increase it up to the highest measurement temperature. That way we obtain, for each set of data, curves of parameters A , B and the correlation coefficient R versus the regression maximum temperature. We thus observe that A , B and R generally start to change from a regression maximum temperature of about 1400 K. We thus conclude that the simple phonon conduction model can be used up to 1400 K. For higher temperatures, electronic and (or) radiative contributions cannot be neglected anymore.

We make the assumption that the validity of the Kopp's law used to calculate the specific heat C_p , which as been experimentally demonstrated for the low Pu content MOX fuels up to 1573 K, can be extended to the whole temperature range covered by our diffusivity measurements.

Therefore, we perform a high temperature quantitative analysis of the data obtained with the reference samples: we first subtract to each experimental data set the phonon contribution, given by the initial $1/(A + BT)$ fit (A and B values of Table 2). We obtain in this way 15 sets of high temperature contribution data points.

Two data sets ([15% Pu, O/M = 1.984] and [10% Pu, O/M = 1.986]) are somewhat higher than the others. This can be seen in Fig. 5(c) and (d) where the triangles are higher than the other data points at high temperature. Such a specific behaviour is not understood. With the exception of these two peculiar sets, all the data lie within a $\pm 5\%$ interval, and show no obvious dependence with the Pu content and the O/M ratio.

All the 15 high temperature contribution data points sets are plotted in Fig. 10 without distinction of the different O/M and the different Pu content, and compared to the high temperature contributions of the FBR recommendation [5] and of the Harding and Martin recommendation for UO_2 [12]. Neither one nor the other high temperature contribution of these two recommendations appears to be suited to describe our data.

A fit of our data with an analytical function of the form $\lambda(T) = aT^3$, which is the form chosen for the FBR recommendation does not give satisfaction. A $\lambda(T) = (C/T^2) \exp(-D/T)$ function, as used by Harding and Martin for their UO_2 recommendation, appears to be much better suited to fit our data. This could be indicative that the high temperature thermal

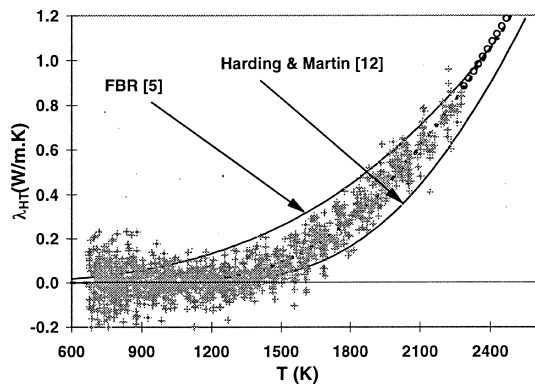


Fig. 10. High temperature contribution conductivity data for the reference fuels, all %Pu and all O/M ratios. The dashed line is a least square fit with a $(C/T^2) \exp(-D/T)$ function. The full lines are the high temperature contributions of the two specified recommendations. The open circles are calculated data (see text).

conduction of our mixed oxide pellets is dominated by electronic conduction, as it has been demonstrated by Young for UO_2 [32].

A least square fit of our data leads to $C = 1.689 \times 10^9 \text{ W K m}^{-1}$ and $D = 3520 \text{ K}$ and a correlation coefficient $R = 0.93$. We thus propose to use the following relation to describe the high temperature conductivity contribution of low Pu content mixed (U,Pu) O_2 oxides:

$$\lambda_{\text{HT}}(T) = (1.689 \times 10^9 / T^2) \exp(-13520/T). \quad (6)$$

It should be remembered that this high temperature analysis is based on the hypothesis of the validity at high temperature of the Kopp's law used to calculate the heat capacity of our samples. Experimental data are needed to confirm or not this hypothesis.

The thermal conductivity of our reference fuels might then be described in the whole temperature range by the equation:

$$\lambda(T) = [(2.85x + 0.035) + (-7.15x + 2.86) \times 10^{-4}T]^{-1} + (1.689 \times 10^9 / T^2) \exp(-13520/T), \quad (7)$$

$x = 2 - \text{O/M}$ being the deviation from stoichiometry and T the temperature in Kelvin.

As an example, Eq. (7) is compared to our experimental data for the 15% Pu content batch in Fig. 11. Note that the apparent discrepancy in the low temperature range between the data and the relation for the [15% Pu, O/M = 1.974] set corresponds to a relative mean difference of only 4.1%, the relation predicting slightly lower conductivity values than those measured.

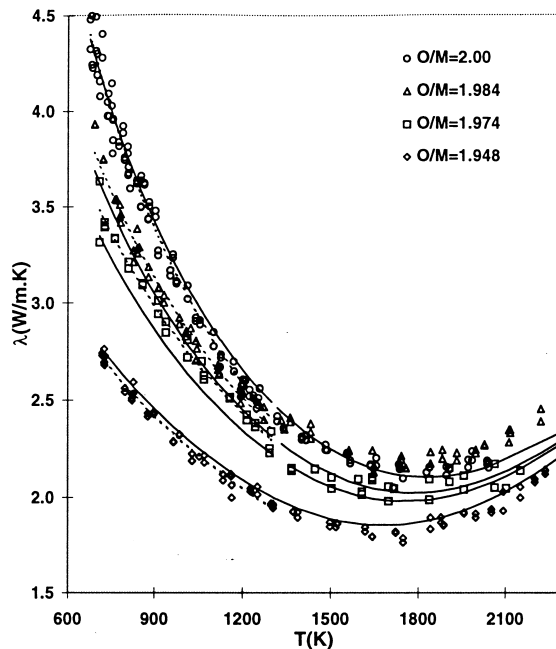


Fig. 11. Comparison of the proposed conductivity relation with the experimental conductivity data for the 15% Pu batch. Full lines: conductivity calculated by Eq. (7). Dashed lines: $1/(A + BT)$ fit of the experimental data (up to 1300 K).

7. Comparison with conductivity of industrial type fuels

The data used to establish Eq. (7) were obtained by measurements with specially prepared samples, hereafter referred as reference fuel samples. They have been annealed for 240 h at 1700°C. Their composition corresponds to an homogeneous solid solution and their microstructure presents unusually high grain size compared to the current fuels obtained with a short sintering time. We should wonder whether this peculiar microstructure could affect the thermal properties and whether our relation could be representative of more conventional industrial fuels.

We then made a few measurements with mixed oxides prepared by the MIMAS process currently used in the French fuel fabrication plants. This process is based on a dry route two stage powder mixing. The obtained pellets present a non-homogeneous plutonium distribution. They can be assimilated as composite fuels: Pu rich master blend agglomerates with size up to about 100 μm are dispersed in a nearly pure UO_2 matrix. The main characteristics (density and mean Pu concentration) of the batches used are given in Table 4.

For this comparison, we included measurements obtained with laboratory prepared MIMAS type fuels (hereafter referred as MIMAS y , where y is the round Pu weight percent) as well as real industrial batches

Table 4
Main characteristics of the ‘industrial type’ batches

Batch	MIMAS 3	MIMAS 6	MIMAS 10	IND1	IND2
Measured Pu content (wt%)	3.09	6.06	10.20	5.9	7.87
d_m/d_{th}	0.96	0.951	0.96	0.947	0.945
Porosity (%)	4	4.9	4	5.3	5.5
O/M ratio after sintering	2.00	2.00	2.00	2.00	1.998

(referred as IND1 and IND2) representative of conventional batches from two different plants. Only one set of measurements was performed with hypostoichiometric samples. It concerns the 6% Pu laboratory prepared batch. One pellet was reduced to $O/M = 1.986$ by the process already used for the reference fuels (reduction at 1700°C under a dry Ar + 5% H_2 flow). The O/M ratio was determined by thermogravimetry (measurement of the weight change during equilibration at 900°C with an Ar + 5% H_2 + 0.2% H_2O atmosphere).

As for the reference samples, we have used, for a given batch, 2 or 3 different disks from the same pellet for the diffusivity measurements. The measured diffusivity values are converted into conductivity data by the method already described in Section 3. The results are given in Figs. 12 and 13 and compared with the new proposed relation and the FBR recommendation [5]. A quantitative comparison is also done by calculating for each set of measurements the relative mean difference $\langle\Delta\lambda/\lambda\rangle$ in the low temperature range as described in

Section 6.1. Results are given in Table 5. It can be seen that as for the reference fuels, the FBR recommendation and our relation both agree quite well with the data on stoichiometric sample. The apparent discrepancy between the FBR recommendation and the IND2 data ($\langle\Delta\lambda/\lambda\rangle = 5.32\%$) is due to the fact that in this case, we have calculated the FBR recommendation for $O/M = 1.998$. In fact, the measured deviation from stoichiometry for the IND2 batch is within the uncertainty of the thermogravimetric method used. We should rather consider that the samples were stoichiometric. The $\langle\Delta\lambda/\lambda\rangle$ then falls to 1.82% if the FBR recommendation is calculated for $O/M = 2.00$. For the set from the MIMAS 6 hypostoichiometric samples, the FBR recommendation overestimates the conductivity decrease, when our relation is in very good agreement with the data.

Therefore, it seems that our relation is well suited for MOX fuels with non-homogeneous plutonium distribution. However, as we only have obtained one

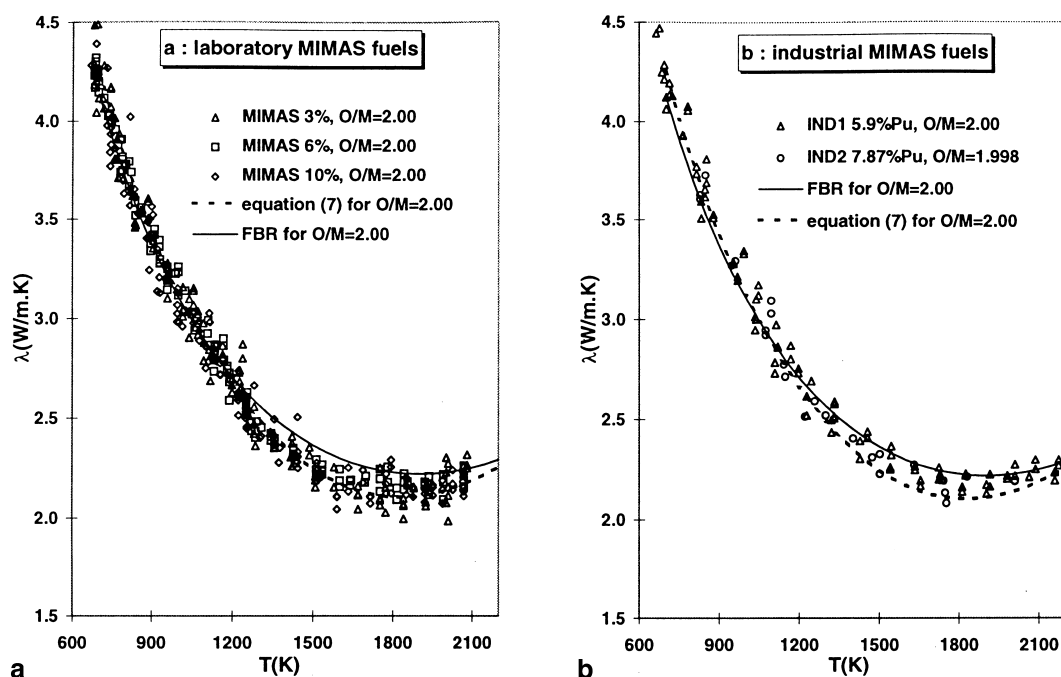


Fig. 12. Conductivity data for the industrial type MIMAS fuels: stoichiometric state.

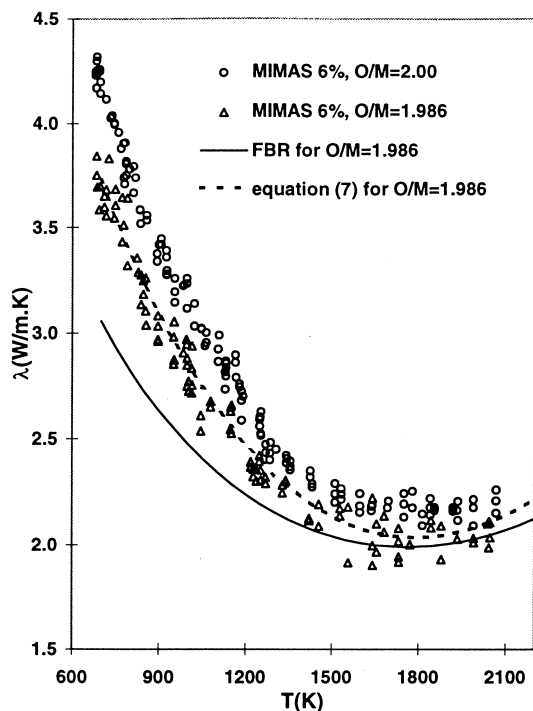


Fig. 13. Conductivity data for the MIMAS 6% Pu laboratory batch.

Table 5

Relative mean differences $\langle \Delta\lambda/\lambda \rangle$ (in %), calculated in the range 700–1300 K (see text), between the relation (5) and the fits on the experimental data for the ‘industrial type’ batches

Batch	O/M	$\langle \Delta\lambda/\lambda \rangle$	
		Present recom.	FBR recom.
MIMAS 3	2.00	1.91	2.10
MIMAS 6	2.00	0.76	1.21
	1.986	0.76	12.15
MIMAS 10	2.00	1.01	1.02
IND1	2.00	1.42	1.77
IND2	1.998	2.27	5.32

measurement set on hypostoichiometric ‘industrial type’ samples, it should be desirable to perform new measurements to definitely conclude that our relation can be used for that kind of fuel.

8. Validity ranges of the proposed conductivity equation

8.1. Temperature range

The low temperature reactor working range is covered by our diffusivity and heat capacity measurements.

In this domain, the conductivity of $(U,Pu)O_{2-x}$ mixed oxides has been shown to be dominated by phonon conduction and Eq. (5) should be well suited to account for the effect of the O/M ratio on the phonon conductivity decrease.

The high temperature limit. our diffusivity measurements cover the range 700–2200 K. It is observed that from about 2000 K, the diffusivity data reach a $\sim 0.55 \times 10^{-6} \text{ m}^2/\text{s}$ value and do not change anymore in the range investigated. Assuming a constant diffusivity value of $0.55 \times 10^{-6} \text{ m}^2/\text{s}$ at high temperature, conductivity data might be calculated outside the temperature range covered by the diffusivity measurements. These data, plotted as open circle in Fig. 10 after subtraction of the phononic contribution given by Eq. (5), appear to keep in good agreement with the proposed conductivity relation (6). However, the Kopp’s law used to calculate the heat capacity has not been experimentally validated at high T and does not take into account the possible existence of an order–disorder transition in the anion sublattice, which would result in a heat capacity peak. Such a phase transition has been theoretically predicted by Bredig [33] and further highlighted for UO_2 at 2670 K from drop calorimetry enthalpy measurements [34,35]. The occurrence of such a transition for $(U,Pu)O_2$ mixed oxides is still not clear, even if Fink have shown that the best fit on existing enthalpy data for 20% and 25% Pu mixed oxide is obtained by postulating that a phase transition occurs at $2750 \pm 50 \text{ K}$ [34]. As far as we are aware, there is no, for low Pu content mixed oxide, high temperature enthalpy data in the literature. A drop calorimetry program is actually in progress in our laboratory to try to reduce this lack of knowledge. Thus, we do not recommend using Eq. (7) above 2600 K.

8.2. Pu concentration range

We have used for this study samples with Pu concentration ranging from 3% to 15%.

The low Pu content limit. It is observed that the conductivity data obtained with the stoichiometric mixed oxide samples are significantly lower than the Harding and Martin recommendation for UO_2 . This finds expression in the B values that are somewhat higher than the B value recommended by Harding and Martin for UO_2 , and indicates that even a small amount of Pu induces a noticeable decrease of the conductivity. However, it is not obvious to determine the minimum Pu concentration for which an effect will be observed, and Eq. (7) should not be used for a Pu concentration lower than the minimum concentration we have experimentally investigated.

The high Pu content limit. It is quite surprising that results obtained with the 15% Pu content MOX samples are so different from what was observed with 20% Pu

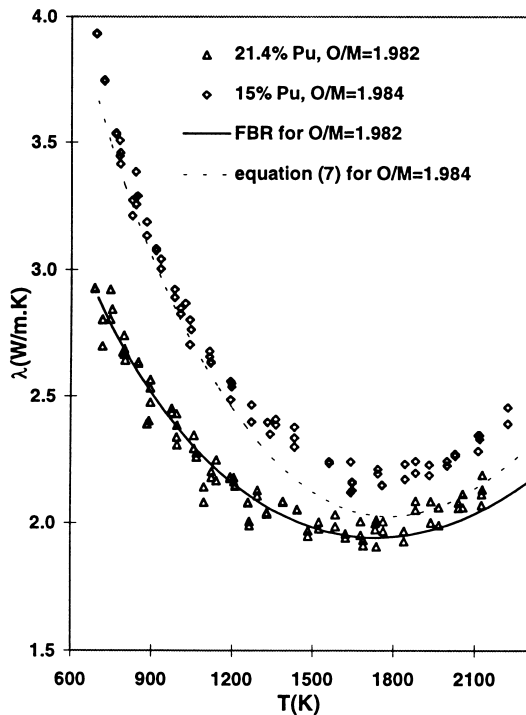


Fig. 14. Comparison of thermal conductivity data for the 15% Pu batch and a 21.4% Pu FBR fuel, for roughly the same deviation from stoichiometry ($O/M \sim 1.98$).

content FBR fuels. To check whether any experimental artefact could have occurred, we have performed a new set of measurements with a FBR batch containing 21.4% Pu. The O/M ratio was 1.982. The behaviour difference between FBR and PWR mixed oxides fuels is obviously confirmed, as can be seen in Fig. 14, where data from this 21.4% Pu batch are compared with the [15% Pu, $O/M = 1.984$] measurement set. The agreement between the 21.4% Pu data and the European FBR recommendation [5] is very good. Therefore, we conclude that Eq. (7) should not be used to calculate the conductivity of hypostoichiometric mixed oxides if the Pu concentration is higher than 15%.

9. Conclusion

We have used the laser flash method and specially prepared homogeneous samples to determine the thermal conductivity of low Pu content $(U_{1-y}, Pu_y)O_{2-x}$ mixed oxides in the ranges $0.03 \leq y \leq 0.15$ and $1.95 \leq x \leq 2.00$. The results satisfy the hyperbolic relationship $\lambda = 1/(A + BT)$, characteristic of a pure phonon conduction mechanism, up to about 1400 K. The A coefficient increases linearly with the deviation from stoichiometry. This can be explained by Abeles simpli-

fied theory for phonon diffusion by point defects, considering the hypostoichiometric oxide as a solid solution of oxygen vacancies in the $(U,Pu)O_2$ lattice and the diffusion centres to be the U^{4+} , Pu^{4+} and Pu^{3+} cations, the O^{2-} anions and the oxygen vacancies. We obtain a strain parameter about four times smaller than for solid solutions of a rare earth or a foreign actinide in an actinide oxide.

Above 1400 K, a high temperature contribution have to be take into account. $A(C/T^2) \exp(-D/T)$ function appears to fit well our data.

For calculation codes purposes, we propose to use the following relationship to describe the thermal conductivity of unirradiated low Pu content mixed $(U,Pu)O_{2-x}$ oxides:

$$\lambda_{95\%} = \lambda_{ph} + \lambda_{HT} = 1/(A + BT) + (C/T^2) \exp(-D/T)$$

with

$$A = A(x) = 2.85x + 0.035 \text{ m K/W,}$$

$$B = B(x) = (-7.15x + 2.86) \times 10^{-4} \text{ m/W,}$$

$$C = 1.689 \times 10^9 \text{ W K m}^{-1},$$

$$D = 13520 \text{ K,}$$

in the range

$$700 \text{ K} \leq T \leq 2600 \text{ K,}$$

$$3\% \leq \text{Pu}/(\text{U} + \text{Pu}) \leq 15\%.$$

This is for 95% dense solid (5% total porosity). The modified Maxwell–Eucken model should be used to correct the porosity effect: the conductivity for a solid with a fractional porosity p is calculated by multiplying the 95% dense conductivity by $f(p)/f(0.05)$, with $f(p) = (1 - p)/(1 + 2p)$.

Acknowledgements

This work was sponsored by EDF and Framatome. We gratefully acknowledge Messrs G. Chaigne and A. Chotard for their constant interest during this work. We also would like to thank Drs M. Beauvy, Y. Guerin and Mr M. Staicu for helpful discussions.

References

- [1] A.B.G. Washington, UKAEA, TRG Report 2236, 1973.
- [2] D.G. Martin, J. Nucl. Mater. 110 (1982) 72.
- [3] Y. Philipponneau, J. Nucl. Mater. 188 (1992) 194.
- [4] J.M. Bonnerot, thesis, CEA Report R-54-60, 1988.
- [5] Fast Reactor Data Manual, issue 1, November 1990.
- [6] T. Ohmichi, S. Fukushima, A. Maeda, H. Watanabe, J. Nucl. Mater. 102 (1982) 40.
- [7] A. Bayoglu, thesis, Orsay, 1981.

- [8] A. Degiovanni, thesis No. 75.19, Université Claude Bernard, Lyon, 1975.
- [9] M. De Franco, J.P. Gatesoupe, in: Fifth International Conference on Plutonium and Other Actinides, Baden-Baden, R.F.A., 10–13 September 1975.
- [10] D.G. Martin, *J. Nucl. Mater.* 152 (1988) 94.
- [11] T. Gervais, Y. Philipponneau, Internal CEA report.
- [12] J.H. Harding, D.G. Martin, *J. Nucl. Mater.* 166 (1989) 223.
- [13] G. Liebfried, E. Schölmann, *E. Akad. Wiss. Gottingen, Math. Physik. K1 (2-A)* (1954) 71.
- [14] Y. Ambegaoker, *Trans. Am. Nucl. Soc.* 9 (1966) 488.
- [15] B. Abeles, *Phys. Rev.* 131 (1963) 507.
- [16] R.L. Gibby, *J. Nucl. Mater.* 38 (1971) 163.
- [17] S. Fukushima, T. Ohmichi, A. Maeda, H. Watanabe, *J. Nucl. Mater.* 102 (1981) 30.
- [18] S. Fukushima, T. Ohmichi, A. Maeda, H. Watanabe, *J. Nucl. Mater.* 105 (1982) 201.
- [19] S. Fukushima, T. Ohmichi, A. Maeda, M. Handa, *J. Nucl. Mater.* 114 (1983) 260.
- [20] S. Fukushima, T. Ohmichi, A. Maeda, M. Handa, *J. Nucl. Mater.* 115 (1983) 118.
- [21] S. Fukushima et al., *J. Nucl. Mater.* 116 (1983) 287.
- [22] S. Fukushima, T. Ohmichi, M. Handa, *J. Less Common Met.* 121 (1986) 631.
- [23] P.S. Murti, C.K. Mathews, *High Temp.-High Press.* 22 (1990) 379.
- [24] S. Ishimoto, M. Hirai, K. Ito, Y. Korei, *J. Nucl. Sci. Technol* 31 (8) (1994) 796.
- [25] M. Amaya, M. Hirai, T. Kubo, Y. Korei, *J. Nucl. Mater.* 231 (1996) 29.
- [26] R.D. Shanon, *Acta Crystallogr. A* 32 (1976) 751.
- [27] B.T.M. Willis, *Proc. Roy. Soc. London A* 274 (1963) 134.
- [28] J.B. Ainscough, M.J. Wheeler, *Brit. J. Appl. Phys. Ser. 2* (1) (1968) 853.
- [29] F.A. Lindemann, *Phys. Z.* 11 (1910) 609.
- [30] W.L. Lyon, W.E. Baily, *J. Nucl. Mater* 22 (1967) 332.
- [31] E.A. Aitken, S.K. Evans, GEAP 5672, 1968.
- [32] R.A. Young, *J. Nucl. Mater* 87 (1979) 283.
- [33] M.A. Bredig, L'étude des transformations cristallines à hautes températures, in: Proceedings of the Conference held in Odeillo, France, 1971 (CNRS, Paris, 1972), p. 183.
- [34] J.K. Fink, *Int. J. Thermophys.* 3 (2) (1982) 165.
- [35] G.J. Hyland, R.W. Ohse, *J. Nucl. Mater.* 140 (1986) 149.